

Research Article

Structural Morphology of Organic Waste-derived Fiber in X-band Frequency

Sirajo Abdullahi* and Yahya Abubakar Aliero

KSUST, Aliero, Nigeria

Abstract

Sawdust is a by-product or waste product of woodworking such as cutting, sanding, machining, planning, and routing. Saw dust consists of small woodcutting intending to study the structural morphology of organic waste fiber derived in an X-band frequency and synthesis of the rice dust and sawdust. The solid-state method was employed to mix the husk, to obtain the fine power, and the Fourier-transform infrared spectroscope was used to determine the sample absorption rate. The FTIR results show that the best samples are 6.5 g and 6.5 g rice bark and sawdust, with an absorbance rate of 86% and 14% transmission, which will be used for the manufacture of electronic and communication devices.

Introduction

Background of the study

Study Sawdust (wood shavings) is a byproduct or waste of woodworking operations such as cutting, sanding, grinding, planning, and routing. It consists of small pieces of wood. These operations can be performed with woodworking machines, portable power tools, or with hand tools. Wood dust is also a by-product of certain animals, birds, and insects living in wood, such as wood pests and carpenters. In some manufacturing industries, it is a major source of fire hazards and exposure to occupational dust [1]. Sawdust is the main component of the particle board. Wood dust is a form of particles. Research on health risks associated with wood dust is carried out in the field of occupational health sciences, and research on wood dust control is carried out in the field of indoor air quality engineering. Rice is one of the most economically important foods in the world today. FAO has reported that it would be beneficial to manage rice processing and its resulting by-products for various reasons in a more sustainable manner. Rice processing involves several grinding stages to produce edible final products. The grinding process is the most important step in rice production, as it determines the nutritional, cooking, and sensory quality of raw rice. When crude rice is processed, by-products such as bran are produced, which have shown beneficial effects on human and animal nutrition [2]. Although some of the rice by-products are used in agriculture, rice bran has probably received the most attention for its functional properties. Rice flour is a

mixture of proteins, fats, dust, and raw fibers. However, the composition of rice bran depends largely on the type of rice and the efficiency of the milling system. Based on mouse studies, it has been shown that rice bran produces prebiotic properties by preventing the colonization of Salmonella in the gastrointestinal tract. In recent years, in vitro incubation studies with chicken ketone contents have shown that some rice varieties are more resistant to Salmonella than others. Furthermore, by-products of rice production can also provide an economic boost to rice-producing countries. This review discusses the by-products of the milling process, how they are used, and the potential applications for rice milling by-products [3].

Meanwhile, it is not hesitating to determine the x-band frequency of rice husk as it is one of the most abundant materials in Nigeria without being processed. X-band frequency range is a part of the microwave spectrum, typically spanning from 8 GHz to 12 GHz. This frequency range is used in many applications that include: radar technology, material characterizations, and satellite communications. In material characterization, x-band frequency is used in studying the dielectric properties of materials such as; Dielectric constant, loss tangent, and permittivity. However, it is essential to determine the molecular and chemical composition of materials in the field of material sciences, therefore FTIR spectrum machine was used to analyze the functional groups, chemical bonds, and molecular structures to provide valuable information about the molecular structure, chemical compositions and physical properties of materials.

More Information

*Address for correspondence: Sirajo Abdullahi, KSUST, Aliero, Nigeria, Email: Abdullahis118@gmail.com

Submitted: February 23, 2023

Approved: June 04, 2024

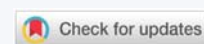
Published: June 05, 2024

How to cite this article: Abdullahi S, Aliero YA. Structural Morphology of Organic Waste-derived Fiber in X-band Frequency. Int J Phys Res Appl. 2024; 7: 066-069.

DOI: 10.29328/journal.ijpra.1001086

Copyright license: © 2024 Abdullahi S, et al. This is an open access article distributed under the Creative Commons Attribution License, which permits unrestricted use, distribution, and reproduction in any medium, provided the original work is properly cited.

Keywords: Organic waste; Fiber; Frequency; Motion; Sawdust



The study was limited to only FTIR analysis to know the chemical composition and find the molecular bonds of the prepared material it was recommended that future research will determine thermal analyses, dielectric spectrometry analyses (electrical conductivity/resistivity, dielectric constants), morphological analysis (Scanning Electron Microscope).

Sónia, et al. (2017), focus on the production by powder metallurgy of aluminum and nickel matrix composites reinforced by CNTs, using ultra-sonication as the dispersion and mixture process. Microstructural characterization of nano-composites was performed by optical microscopy (OM), scanning and transmission electron microscopy (SEM and TEM), electron backscattered diffraction (EBSD), and high-resolution transmission electron microscopy (HRTEM). Microstructural characterization revealed that the use of ultra-sonication as the dispersion and mixture process in the production of Al/CNT and Ni/CNT nano-composites promoted the dispersion and embedding of individual CNT in the metallic matrices. CNT clusters at grain boundary junctions were also observed. The strengthening effect of the CNTs is shown by the increase in hardness for all nanocomposites. The highest hardness values were observed for Al/CNT and Ni/CNT nanocomposites, with a vol% CNTs.

Konakov, et al. (2017) report on the detailed study of graphene-modified bulk nickel composites with a phase content of up to 4.7% of graphene+graphite. The composites were manufactured dusting ball milling and powder metallurgy methods, nickel nanopowder, and exfoliated graphite as the starting materials. Phase composition and composite structures were investigated using X-ray diffraction (XRD), differential scanning calorimetry (DSC), Raman spectroscopy (RS), and scanning electron microscopy (SEM). The effect of adding graphene on grain size and orientation was determined from electron images (EBSD technology). The effect of the content of graphene-graphite phases on the mechanical properties of the composite was studied. It has been shown that small amounts of this phase produce the formation of graphs on the surface of metal grains, which in turn affects the mechanical properties of composites: their hardness increases, their plasticity decreases, and the resistance value remains at the same level. The effect of different surfactants on the volume of SiCco-deposition in a nickel matrix was evaluated. Among the various substances investigated, tetramethyl ammonium hydroxide (TMAH) was the best to improve the quality of the deposits and the uniform distribution of particles, with areas on the able amount of silicon carbide content in the matrix. Composites are made using powders and 50 nanometers. The effect of silicon carbide concentration and bath operating variables on SiC incorporation volume in the deposit and deposition rates has been estimated. NanoSiC composites significantly improved mechanical properties, such as hardness and wear resistance, compared to micro Sic composites (Narasimman, et al. 2012).

Materials and methods

Materials

- i. FTIR machine
- ii. Weighing balance
- iii. Rice husk
- iv. Sawdust
- v. Motor and pestle
- vi. Acetone

Sample preparation

Rice husk and wood sawdust were collected from the new market in the city of Aliero. The materials were used and, after a certain leaning, were purified. The material is 99.9% pure. Both, the Motor and pestle, acetone, and weighing balance were manufactured by United Scientific (pty) Ltd. and obtained at the chemical laboratory of Kebbi State University of Science and Technology, Aleiro. While Drawell Instrument Co., Ltd; DW-FTIR-530A spectrometer was obtained at Research Center Sokoto.

Preparation of the sample

The first step was to collect both rice and sawdust for the preparation of the sample. The rice kernel and sawdust were thoroughly washed with acetone and dried at ambient temperature for 48 hours, and then measured on five different samples (0.1, 0.3, 0.5, 0.7, and 0.9) using a weight balance in the chemistry laboratory of the State University of Science and Technology in Kebbi, Aleiro as shown in Table 1. The samples are then mixed with a ceramic motor and a pestle, during the mixing process of a sample, the rotation of the pestle is done in the clockwise direction for 15 minutes during the mixing process of all samples, with constant movement to achieve the homogeneity of the sample.

Sample characterization

A technique has been used for the characterization of electromagnetic properties. The materials are analyzed using Fourier transform Infrared Spectroscopy (FTIR) technology. The molecular composition and structure of the sample were analyzed using the FTIR spectrometer (DW-FTIR-530A) at the National Chemical Research Centre (UDUS) in Sokoto.

Results and discussions

Results obtained from FTIR spectroscopy for 16.7%,

Table 1: Summary of the Sample Compositions.

S/N	Rice husk (g)	Sawdust (g)	Total (g)
1	10.5	2.5	13
2	8.5	4.5	13
3	6.5	6.5	13
4	4.5	8.5	13
5	2.5	10.5	13

25.0%, and 33.3% rice shell and sawdust composites, respectively. It was acquired between 750 and 4000 cm^{-1} in wave number, with a maximum transmission of 100%. Figure 1 FTIR spectrum of rice powder and rice dust observing 0.1 kg and 0.9 kg showed the absorption regions 717.54 cm^{-1} , 825.50 cm^{-1} , 1219.05 cm^{-1} , 1334.78 cm^{-1} , 1681.98 cm^{-1} , and 1774.57 cm^{-1} . The highest observed absorption is 83.3% to 134.78 cm^{-1} , which corresponds to 16.7% of transmission. The absorption band observed at 717.54 cm^{-1} corresponds to C-Cl stretching vibrations and that at 825.50 cm^{-1} asserts C-C skeletal vibrations. The band of 1219.05 cm^{-1} corresponds to the vibrations of C-N expansion. The band that appeared at 1334.78 cm^{-1} is attributed to the vibration of the C-H curve. The band of 1681.98 cm^{-1} corresponds to the symmetric C=O. The band of 1774.57 cm^{-1} is associated with C=O deformation (Assem, et al. 2013).

Figure 2 shows the absorption region of 725.26 cm^{-1} , 763.84 cm^{-1} , 817.85 cm^{-1} , 1219.05 cm^{-1} , 1342.50 cm^{-1} , 1419.00 cm^{-1} , 1512.24 cm^{-1} , 1681.98 cm^{-1} and 1766.85 cm^{-1} . The highest absorbance recorded is around 84.1% at 1512.24 cm^{-1} corresponding to 15.9% of transmittance. The absorption band observed at 725.26 cm^{-1} and 763.84 cm^{-1} corresponds to strong C-Cl stretching. The band at 817.85 cm^{-1} attributes C-C skeletal vibrations. The absorption at 1219.05 cm^{-1} corresponds to C-N stretching vibrations. The band appearing at 1342.50 cm^{-1} is attributed to C-H bending vibration. The band at 1419.00 cm^{-1} corresponds to asymmetric C-H bending. The absorption band at 1512.24 cm^{-1} is attributed to C-H skeletal vibrations. The band at 1681.98 cm^{-1} corresponds to the symmetrical of C=O. The band at 1766.84 cm^{-1} attributes the C=O stretching [4].

Figure 2 shows the absorption area of 725.26 cm^{-1} , 763.84 cm^{-1} , 817.85 cm^{-1} , 1219.05 cm^{-1} , 1342.50 cm^{-1} , 1419.00 cm^{-1} , 1512.24 cm^{-1} , 1681.98 cm^{-1} and 1766.85 cm^{-1} . The highest recorded absorption is around 84.1% , 1512.24 cm^{-1} , corresponding to 15.9% of the transmittance. The absorption bands of 725.26 cm^{-1} and 763.84 cm^{-1} correspond to strong C-Cl elongation. The band of 817.85 cm^{-1} is attributed to C-C skeletal vibrations. The absorption at 1219.05 cm^{-1} corresponds to the C-N extension vibrations. The band appearing at 1342.50 cm^{-1} is attributed to the vibration of the C-H curve. The 1419.00 cm^{-1} band corresponds to an asymmetric C-H curve. The absorption band at 1512.24 cm^{-1} is due to the skeletal vibrations of C-H. The band 1681.98 cm^{-1} corresponds to the symmetric of C=O. The band of 1766.84 cm^{-1} is C=O extended [4]. Figure 2 FTIR spectrum of 8.5g and 4.5g rice dust and sawdust Careful observation of Figure 3 shows the absorption region of 717.54 cm^{-1} , 817.85 cm^{-1} , 1219.05 cm^{-1} , 1342.50 cm^{-1} , 1411.94 cm^{-1} , 1504.53 cm^{-1} , 1658.84 cm^{-1} , 1774.57 cm^{-1} and 3433.41 cm^{-1} . The highest absorption rate observed was 86%, i.e. 1504.53 cm^{-1} , corresponding to 14% of transmission. The absorption band at 717.54 cm^{-1} corresponds to a strong C-Cl extension, and the band at 817.85 cm^{-1} indicates C-C skeletal vibrations. The absorption of 1219.05 cm^{-1} corresponds to C-N

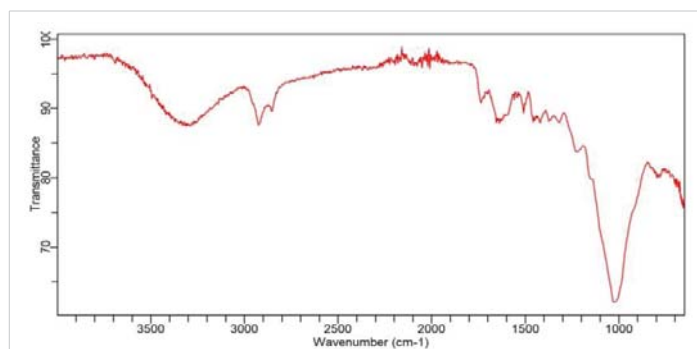


Figure 1: FTIR spectra 3500 to 1000 for 10.5 g and 2.5 g of rice husk and sawdust.

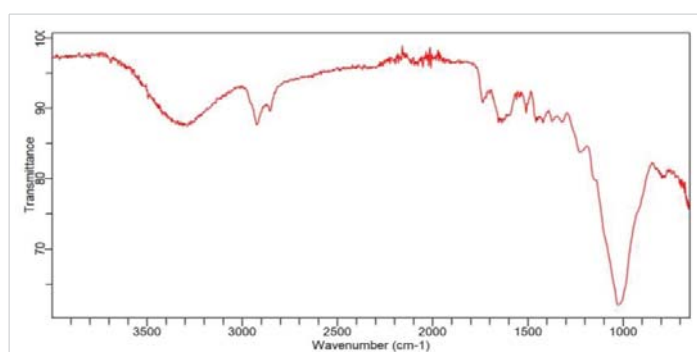


Figure 2: FTIR spectra 3500 to 1000 for 8.5 g and 4.5 g of rice husk and sawdust.

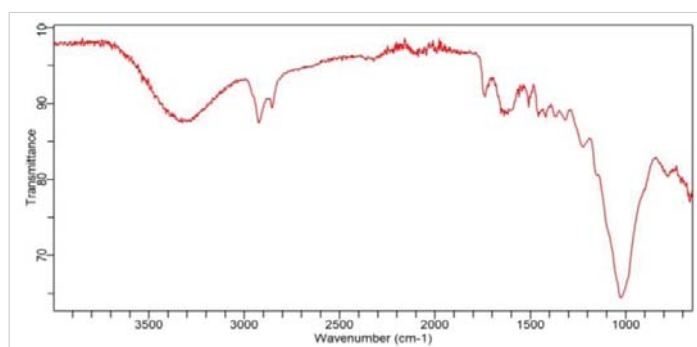


Figure 3: FTIR spectra 3500 to 1000 for 6.5 g and 6.5 g of rice husk and sawdust.

expansion vibrations. The band, which appears at 1342.50 cm^{-1} , is due to C-H bending vibration. The 1411.94 cm^{-1} band corresponds to an asymmetric C-H bend. The band 1658.84 cm^{-1} corresponds to the symmetrical C=O. The 1774.57 cm^{-1} band attributes the extension of C=O and the 3433.41 cm^{-1} corresponds to the strong extension of O-H [5]. The 33.3% waste composite showed the highest absorption, which indicates an increase in absorption as the amount of doping increases.

Figure 4 shows the absorption area 725.26 cm^{-1} , 763.84 cm^{-1} , 817.85 cm^{-1} , 1219.05 cm^{-1} , 1342.50 cm^{-1} , 1419.24 cm^{-1} , 1512.24 cm^{-1} , 1681.98 cm^{-1} and 1766.85 cm^{-1} . The highest recorded absorption rate is around 84.1% at 1512.24 cm^{-1} , corresponding to 15.9% of transmission. The absorption bands of 725.26 cm^{-1} and 763.84 cm^{-1} correspond to a strong C-Cl extension. The band of 817.85 cm^{-1} is attributed to C-C skeletal vibrations. The absorption at 1219.05 cm^{-1} corresponds to the

C-N expansion vibrations. The band that appears at 1342.50 cm^{-1} is attributable to the vibration of the C-H curve. The band of 1419.00 cm^{-1} corresponds to the asymmetric curve of C-H. The absorption band of 1512.24 cm^{-1} is attributed to C-H skeletal vibration. The band 1681.98 cm^{-1} corresponds to the symmetric C=O. The band of 1766.84 cm^{-1} shows the expansion of C=O [5].

Figure 5 FTIR spectrum of 8.5g and 4.5g rice straw and

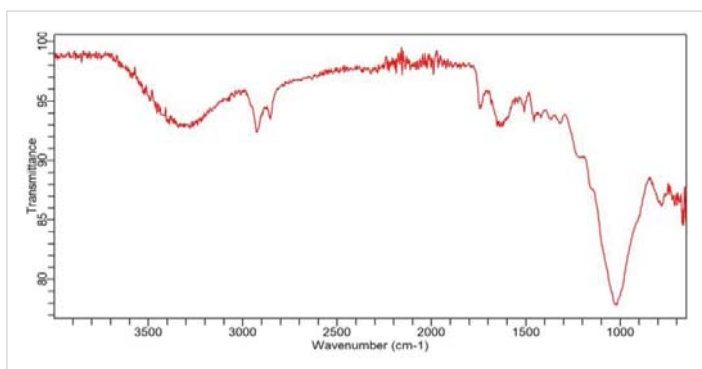


Figure 4: FTIR spectra 3500 to 1000 for 8.5 g and 4.5 g of rice husk and sawdust.

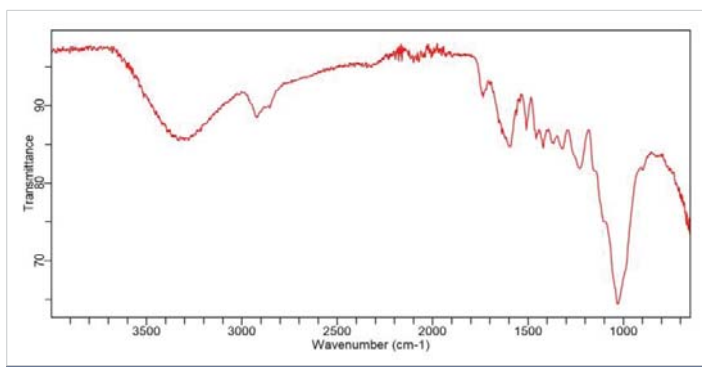


Figure 5: FTIR spectra 3500 to 1000 for 10.5 g and 2.5 g of rice husk and sawdust.

wood dust Observation in Figure 4 the absorption region of 717.54 cm^{-1} , 825.50 cm^{-1} , 1219.05 cm^{-1} , 1334.78 cm^{-1} , 1681.98 cm^{-1} and 1774.57 cm^{-1} . The highest absorbance was observed at 83.3% to 1334.78 cm^{-1} , representing 16.7% of the transmission. The absorption band at 717.54 cm^{-1} corresponds to C-Cl expansion vibrations and the band at 825.50 cm^{-1}

corresponds to C-C skeletal vibrations. The band of 1219.05 cm^{-1} corresponds to the vibrations of C-N stretching. The band that appeared at 1334.78 cm^{-1} is due to C-H bending vibration. The 1681.98 cm^{-1} band corresponds to the symmetry of C=O. The band at 1774.57 cm^{-1} is attributable to the expansion of C=O (Assem, et al. 2013).

Conclusion

The results obtained by FTIR spectroscopy for the transmission of 16.7%, 15.9%, 14%, 15.9%, and 16.6% organic waste products composites, respectively, were obtained. They were obtained in the range of 750 to 4000 cm^{-1} wave, with a maximum absorption rate of 100%. All composites will be used in the construction of electronic devices and also in the telecommunications industries (capacitors and inductors).

Recommendation

It was recommended that relevant characterizations be introduced such as thermal analyses, dielectric spectrometry analyses (electrical conductivity/resistivity, dielectric constants), morphological analyses (SEM), and TEM analyses for future investigations.

References

1. Robert W, Dragan E. Fundamentals of Power Electronics. 2nd ed. Kluwer Academic Publishers; 2001. 5-10.
2. Krishan KC. Composite Materials, Science and Engineering, Third Edition, 12-20. New York Heidelberg Dordrecht London. 2012. ISBN 978-0-387-74364-6 ISBN 978-0-387-74365-3 (Ebook) DOI 10.1007/978-0-387-74365-3.
3. Sonnia ENM, ling TB, Png LS By-products of Rice Processing: an overview of health benefits and application. Rice Res. 2013; 1:1-11
4. Yakubu A, Ahmad F, Zulkifly A, Mohamad ZF, Suzan J. Dielectric Characterization of Oil Palm Fiber Reinforced Polycaprolactone Nickel Oxide Composite At Microwave. Procedia Environment Science. 2015; 30:273-278.
5. Yakubu A, Zulkifly A, Nor A, Ibrahim, Ahmad F. Reduction of Electromagnetic Interference Using ZnO-PCL Nanocomposites at Microwave Frequency. Advances in Materials Science and Engineering. 2015;4:7. Article ID 132509.